

## Shape descriptors for mode-shape recognition and model updating

This content has been downloaded from IOPscience. Please scroll down to see the full text.

2009 J. Phys.: Conf. Ser. 181 012004

(<http://iopscience.iop.org/1742-6596/181/1/012004>)

View [the table of contents for this issue](#), or go to the [journal homepage](#) for more

Download details:

IP Address: 134.83.1.242

This content was downloaded on 11/05/2015 at 14:30

Please note that [terms and conditions apply](#).

## Shape descriptors for mode-shape recognition and model updating

Weizhuo Wang<sup>1</sup>, John E Mottershead<sup>1,†</sup> and Cristinel Mares<sup>2</sup>

<sup>1</sup>Department of Engineering, The University of Liverpool, Liverpool, UK, L69 3GH

<sup>2</sup>School of Engineering and Design, Brunel University, Middlesex, UK, UB8 3PH

† [j.e.mottershead@liverpool.ac.uk](mailto:j.e.mottershead@liverpool.ac.uk)

**Abstract.** The most widely used method for comparing mode shapes from finite elements and experimental measurements is the Modal Assurance Criterion (MAC), which returns a single numerical value and carries no explicit information on shape features. New techniques, based on image processing (IP) and pattern recognition (PR) are described in this paper. The Zernike moment descriptor (ZMD), Fourier descriptor (FD), and wavelet descriptor (WD), presented in this article, are the most popular shape descriptors having properties that include efficiency of expression, robustness to noise, invariance to geometric transformation and rotation, separation of local and global shape features and computational efficiency. The comparison of mode shapes is readily achieved by assembling the shape features of each mode shape into multi-dimensional shape feature vectors (SFVs) and determining the distances separating them.

### 1 Introduction

Accurate vibration mode shape information is available for large and complicated structures by using modern computational finite element methods and full-field optical measurement technique [1]. *Image processing* (IP) and *pattern recognition* (PR), well developed in other disciplines, enables the versatile comparison and classification of mode shapes [2, 3], which cannot be achieved by the conventional *Modal Assurance Criterion* (MAC) [4]. A set of shape features with good discriminative capability may be extracted by IP and PR methods to form a feature vector – *shape descriptor* (SD). Now the similarity/dissimilarity of the shapes can be revealed by the ‘distance’ of their corresponding SDs in the shape feature space according to appropriate criteria.

The moment descriptor is one of the most popular shape descriptors in image processing and pattern recognition [5] but the non-orthogonality of the moment basis gives rise to redundancy and the original shape generally becomes difficult to recover from a truncated set of moment descriptors. Teague [6] suggested using orthogonal polynomials to replace the algebraic polynomials when calculating the moment descriptor.

The *Zernike moment* (ZM) is based on a complete set of orthogonal polynomials over a circle of unit radius – Zernike polynomials. It was found later that the Zernike moment is one of the most important region-based shape descriptors because of its outstanding properties resulting from the orthogonality of the Zernike polynomials. Firstly, expressing an image as a set of mutually independent descriptors has the effect of minimising the redundancy of information. Secondly, the contribution of each order of moment to the image reconstruction can be separated, so that the process

of regaining the original image is much easier than by geometric moment descriptors [7]. Rotational invariance [8, 9] is another important property of the ZM, meaning that rotating an image does not change the magnitudes of its Zernike moments. Also, the ZM is robust to noise [7] and effective, meaning that a small number of Zernike moments are usually sufficient for shape reconstruction. The ZM in vibration mode-shape recognition is described in detail by the present authors [10].

*Fourier Descriptors* (FDs) were originally proposed in 1960 by Cosgriff [11], and thereafter became popular among the pattern recognition community through the papers of Zahn [12], Persoon and Fu [13]. FDs are among the most popular shape representation methods for vision and pattern recognition applications. FDs refer to a class of methods, not a single method, since there are many different ways in which the FDs of a shape can be defined. The basic idea underlying this approach consists in representing the shape of interest in terms of a 1D, 2D or even 3D signal. The Fourier transform of this signal is determined and the FDs are calculated for this Fourier representation. Some properties of the FDs directly follow from the underlying theory of the Fourier transforms and series. For instance, the 0<sup>th</sup> component of the FDs obtained from the contour representation is associated with the centroid of the original shape. The invariance to geometric transformations is also a direct consequence of the properties of the Fourier series. Such properties have helped to popularize this shape representation scheme, which has been adopted in a number of applications during the last four decades.

In certain applications, local shape information is particularly significant, when certain shape features are associated with a particular portion of the object, such as a discontinuity, singularity or local frequency. *The Short-Time Fourier descriptor* (SFD) [14] and *Wavelet descriptor* (WD) [15] are two of the most powerful method for detecting local shape features, especially the WD. An important property of the wavelet descriptor is its ability to separate local features from the global shape, while avoiding the problem of a local modification affecting the whole representation. For example a partial occlusion may interfere significantly with a global shape descriptor, such as the Fourier descriptor or moment descriptor, while the wavelet descriptor of the unblocked part is not affected at all. The FD and WD in vibration mode-shape recognition are described in detail by the present authors [16].

Thus, a *shape feature vector* (SFV) can be formed by assembling the different SDs. The comparison of mode shapes is then transformed to the similarity measurement between the SFVs in the feature space. Dimensionless normalisation for the SFV is necessary before commencing the comparison to avoid the scaling effect.

## 2 Shape Descriptors

The theory of the various shape descriptors is described in full by the present authors [10, 16]. A brief outline of the theory is provided in this article. The general form of SDs may be expressed as,

$$\mathcal{D} = \mathcal{T}[I(x, y)] \quad (2-1)$$

where  $I(x, y)$  denotes the continuous displacement mode shape function and  $\mathcal{T}[*]$  represents the transformation for extracting the shape features. More specifically, the SD can be defined by projecting the image function onto a kernel function  $\mathfrak{K}(x, y)$  as

$$\mathcal{D} = \int_{\Omega} \mathfrak{K}(x, y) I(x, y) dx dy \quad (2-2)$$

where  $\Omega$  denotes the domain of definition. Different types of SDs (ZMs, FDs, WDs etc.) are defined by using different kernel functions.

### 2.1 Zernike Moment Descriptor

A set of two-dimensional complex polynomials defined over a unit circle was introduced by Zernike [17], written as

$$V_{n,m}(x, y) = V_{n,m}(\rho, \vartheta) = R_{n,m}(\rho) e^{im\vartheta} \quad (2-3)$$

where  $i = \sqrt{-1}$ ,  $(\rho, \vartheta)$  is the polar coordinate,  $n$  is the non-negative integer, representing the order

of the radial polynomial,  $m$  denotes the positive / negative integer subject to constraints  $n - |m|$  even,  $|m| \leq n$  (representing the repetition of the azimuthal angle) and  $R_{n,m}$  is the radial polynomial defined as [17],

$$R_{n,m}(\rho) = \sum_{s=0}^{\frac{n-|m|}{2}} (-1)^s \frac{(n-s)!}{s! \left(\frac{n+|m|}{2}-s\right)! \left(\frac{n-|m|}{2}-s\right)!} \rho^{n-2s} \quad (2-4)$$

According to the orthogonality properties [18], the inner product of any pair of complex Zernike polynomials can be expressed as

$$\iint_{x^2+y^2 \leq 1} V_{p,q}(x,y) V_{n,m}^*(x,y) dx dy = \frac{\pi}{n+1} \delta_{n,p} \delta_{m,q} \quad (2-5)$$

where \* denotes the complex conjugate and  $\delta_{n,p}$  and  $\delta_{m,q}$  are Kronecker deltas. Thus, the Zernike moment descriptor can be obtained by substituting the Zernike polynomials into the kernel function in (2-2), in polar coordinates as,

$$\mathfrak{D}_{Z_{n,m}} = \frac{n+1}{\pi} \int_0^{2\pi} \int_0^1 I(\rho, \vartheta) V_{n,m}^*(\rho, \vartheta) \rho d\rho d\vartheta \quad (2-6)$$

The original image  $I(\rho, \vartheta)$  may easily be reconstructed by virtue of the orthogonality of the ZMDs. Expression efficiency is one of the important properties of the ZMD, meaning the main shape information may be extracted by the lower order moments after truncating the higher orders of the ZMD in real applications. Rotational invariance is another significant property [9] of the ZMD, useful for recognising mode shapes of axisymmetric structures [10].

## 2.2 Fourier Descriptor

The FD is based on the frequency components from *Fourier transform* (FT) of the images. According to the well-known theory of the FT, the kernel function of the SD is the complex valued sinusoid,

$$\mathfrak{D}_{\mathcal{F}}(u, v) = \int_{-\infty}^{+\infty} \int_{-\infty}^{+\infty} e^{-i2\pi(ux+vy)} I(x, y) dx dy \quad (2-7)$$

$\mathfrak{D}_{\mathcal{F}}(u, v)$  is a continuous function having the same cardinality as  $I(x, y)$ , and for real applications, this needs to be reduced whilst retaining as much information as possible. Generally the low frequency and higher energy components are sufficient to describe the shape. Thus, for instance, elliptical descriptors (such as *centroid*, *orientation*, *eccentricity* and *spread*) based on the FD spectrum are feasible to indicate the distribution of the frequency energy. Also, the FD spectrum can be divided into non-overlapping sub-bands. The average energy from each sub-band then becomes an element of the feature vector. The latter extraction method is easily implemented when applying the *discrete Fourier transform* (DFT),

$$\mathfrak{D}_{\mathcal{F}}(u, v) = \frac{1}{KL} \sum_{k=0}^{K-1} \sum_{\ell=0}^{L-1} e^{-i2\pi\left(\frac{uk}{K} + \frac{v\ell}{L}\right)} I(k, \ell) \quad (2-8)$$

Reconstruction is straight forward by applying the inverse Fourier transform. Good approximation may be obtained by retaining a sufficient number of higher energy terms.

## 2.3 Wavelet Descriptor

The idea of wavelet transformation is to represent an image in terms of the superposition of wavelet with different scale levels and positions. The wavelet, having better time-frequency resolution than *short-time Fourier transform* (STFT) [19], can be expressed as

$$\psi_{b_x, b_y, a} = \frac{1}{a} \psi\left(\frac{x-b_x}{a}, \frac{y-b_y}{a}\right) \quad (2-9)$$

where  $a \in \mathbb{R}^+$  is the dilating scale parameter,  $(b_x, b_y) \in \mathbb{R}^2$  are the translation parameters and  $\psi_{b_x, b_y, a}$  is the translated and dilated version of the mother wavelet  $\psi(x, y)$ . The normalisation factor  $1/a$  is included so that  $\|\psi_{b_x, b_y, a}\| = \|\psi\|$ . Depending on the applications, these parameters can be chosen as either continuous or discrete values. The definition of CWT can be expressed as an inner product of the wavelet and the image,

$$\mathfrak{D}_w(a, b_x, b_y) = \langle \psi_{b_x, b_y, a}, I(x, y) \rangle = \int_{-\infty}^{+\infty} \int_{-\infty}^{+\infty} \psi_{b_x, b_y, a}^*(x, y) I(x, y) dx dy \quad (2-10)$$

The mother wavelet must satisfy

$$\int_{-\infty}^{+\infty} \int_{-\infty}^{+\infty} \psi(x, y) dx dy = 0 \quad (2-11)$$

so that the wavelet is oscillatory with a null DC component.

Discretization of the wavelet parameters is adopted in many applications [19]. We consider the wavelet decomposition of a two-dimensional mode shape. The *two-dimensional discrete wavelet transform* (DWT2) for an image can be obtained by implementing the one-dimensional algorithm horizontally and then vertically. The outputs from each step of decomposition are the sub-images of one approximation at coarser resolution and three sub-images of detail in horizontal, vertical and diagonal directions as illustrated in Fig 1. Thus, the comparison between images can now be carried out between the sub-images at different resolutions. In addition, these coefficients can be used as the WDs and the average energy of each sub-image may be used to form the SFV. A more detailed description of the method is given by the present authors [16].

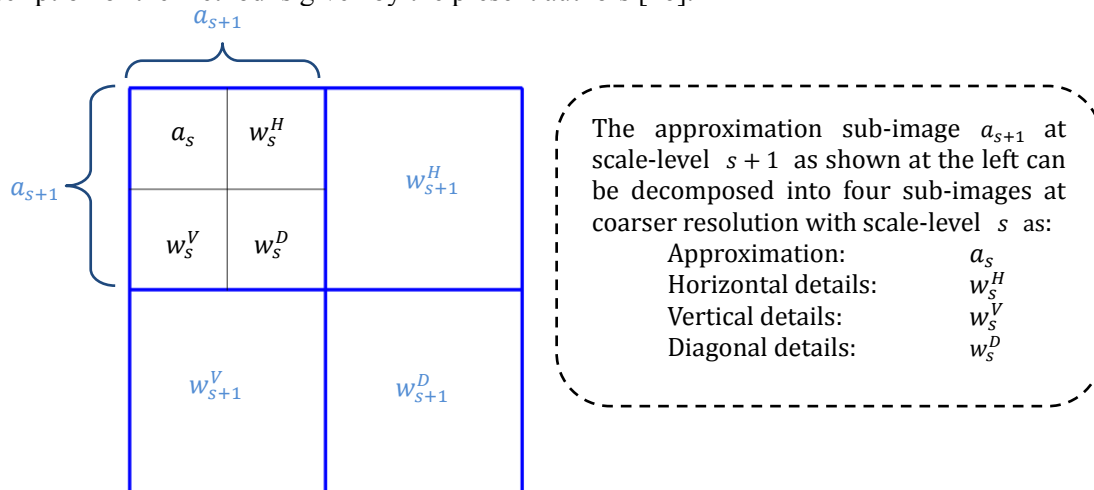


**Fig 1:** Decomposition of Sub-Images between Two Scales

### 3 SD Sensitivity and Model Updating

The deterministic model updating process by the iterative sensitivity method can be written as [20],

$$\theta_{j+1} = \theta_j + [\mathcal{S}_j^T \mathcal{S}_j]^{-1} \mathcal{S}_j^T (z_m - z_j) \quad (3-1)$$

where  $\theta_j$  and  $\theta_{j+1}$  are the structural parameters of the current and next iterative steps;  $\mathcal{S}_j$  denotes the sensitivity matrix at the current iteration;  $z_j$  is the current output and  $z_m$  is the measured output. Here, the output is considered to be the SD rather than the eigenvalues or eigenvectors in the conventional study. Thus, the sensitivity matrix, known as the SD sensitivity matrix, can be calculated by taking the derivatives of SD with respect to the structural parameters. That is,

$$\mathcal{S}_D = \frac{\partial \mathfrak{D}}{\partial \theta} = \frac{\partial [\int_{\Omega} \mathfrak{K}(x, y) I(x, y, \theta) dx dy]}{\partial \theta} \quad (3-2)$$

It is noted that the continuous mode shape function can be determined by a linear combination of a set of pre-described element shape-functions  $\boldsymbol{\pi}(x, y)$  with the eigenvector  $\boldsymbol{\Phi}(\theta)$  as [10]

$$I(x, y, \theta) = \boldsymbol{\pi}^T(x, y) \boldsymbol{\Phi}(\theta) \quad (3-3)$$

Substituting (3-3) into (3-2) and applying the Leibniz integral rule yields

$$\mathcal{S}_D = \left[ \int_{\Omega} \mathfrak{K}(x, y) \boldsymbol{\pi}^T(x, y) dx dy \right] \frac{\boldsymbol{\Phi}(\theta)}{\partial \theta} \quad (3-4)$$

which indicates that the sensitivity of SD may be calculated analytically by multiplying together the SD of the element shape-functions and the sensitivity of eigenvector.

## 4 Examples

### 4.1 ZMD of a Circular Plate

The free vibration of a circular plate can be modelled by finite elements. Since the circular plate is a perfectly axisymmetric structure double modes are obtained. The conventional mode-shape comparison method, MAC, shows nothing about the double modes. Thus, the ZMD is applied to the first 20 modes. As illustrated in Fig 2, only a small number of the lower order ZMDs are needed to represent all the modes. Correlation of mode shapes based on the ZMD amplitudes is shown in Fig 3 where the double modes can be clearly recognised.

Furthermore, the rotational difference between any pair of double modes can be determined by a property of the ZMD [10]. The first pair of double modes 1 and 2 is shown in Fig 4. As seen from Fig 2 their ZMDs are mainly dominated by  $\mathcal{D}_{Z_{2,2}}$ . The angle  $\alpha = (\arg(\mathcal{D}_{Z_{2,2}^{(2)}}) - \arg(\mathcal{D}_{Z_{2,2}^{(1)}}))/2 = \frac{90.1^\circ}{2} = 45.1^\circ$  matches the theoretical angular difference between double modes 1 and 2, shown in Fig 5.

The orthogonality property of the ZMDs means that they are not only excellent shape descriptors but also their sensitivities are powerful in updating finite element models. The same circular plate is now supported by an elastic foundation at the circumference. Two structural parameters, translational stiffness perpendicular to the plate ( $k_w$ ) and rotational stiffness with respect to the tangent of circumference ( $k_a$ ), of the elastic foundation are considered to be updated in this simulation.  $k_w = 1000$  and  $k_a = 2000$  were used to generate the simulated measurements. The initial values of parameters were  $k_w = 700$  and  $k_a = 1500$  in the first updating test and  $k_w = 1500$  and  $k_a = 2500$  in the second test. The ZMD sensitivities were computed using predefined values of the parameters values. The ZMDs of the mode shapes were calculated from orders 0 to 8. The updating parameters converged to the *target* in 4 and 5 iterations respectively as shown in Table 1.

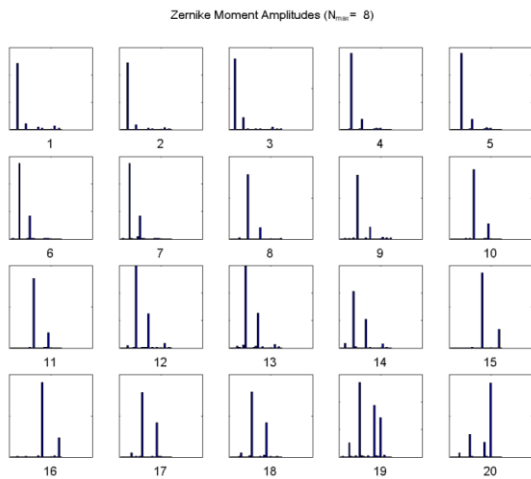


Fig 2: Amplitudes of the ZMDs

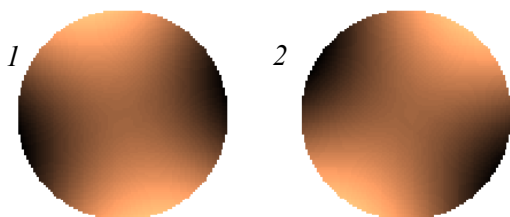


Fig 4: Mode-Shape Patterns of Mode 1 & 2

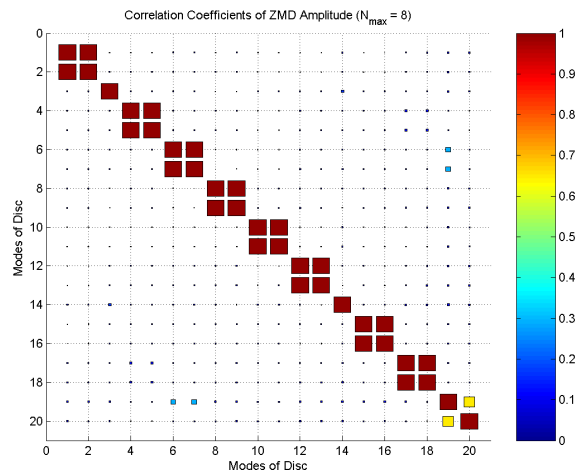


Fig 3: Correlation of the ZMD Amplitude

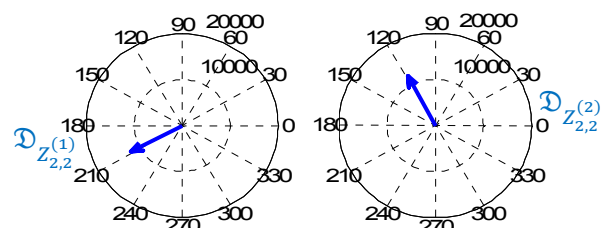


Fig 5: The  $\mathcal{D}_{Z_{2,2}}$  of Modes 1 & 2

*Table 1: Convergence of the Updating Parameters*

	Steps	0	1	2	3	4	5	Target
<b>Test 1</b>	$k_w$	700.00	912.60	993.16	1000.02	1000.00		1000.00
	$k_a$	1500.00	2426.30	2031.40	1999.90	2000.00		2000.00
<b>Test 2</b>	$k_w$	1500.00	753.78	939.57	996.40	999.99	1000.00	1000.00
	$k_a$	2500.00	3119.83	2283.60	2016.91	2000.04	2000.00	2000.00

4.2 FD of a Rectangular Plate

Free vibration of a  $160 \times 120 \times 2mm$  rectangular aluminium thin plate is modelled. The FDs of the mode shapes are determined by the DFT. Fig 6 shows the amplitudes of the FDs for the first 12 modes in the first quadrant. It is noted that only a few lower frequency components are significant. The elliptical descriptors of the spectrum are also presented in the figures, which describe the spectrum pattern globally. A hierarchical clustering algorithm is applied to the elliptical descriptor. Several clusters may be obtained by ‘cutting’ the dendrogram shown in Fig 7 at a chosen distance separating the various groups of modes. The most compact cluster *C1* ((1,7),10) indicates the similarity of the three spectrum patterns as shown in Fig 6. Cluster *C2* ((5,12),6) groups together those modes with a strongly dominant horizontal major axis of the ellipse. Also, the three compact ellipses having horizontal major axes are grouped by cluster *C3* (2,(8,11)). Furthermore, the similarities between FD patterns indicated by these clusters can be referred back to the similarities between mode shapes. The nodal lines of the 12 modes are shown in Fig 8. According to the closeness of mode 1, 7 and 10 (indicated by cluster *C1*) it can be seen from their nodal lines that mode 7 has two more horizontal oscillations than mode 1 whilst mode 10 has two more vertical oscillations than mode 1. For cluster *C2*, mode 12 has two more oscillations than mode 6 horizontally and mode 5 vertically. Similar relations between mode 2, 8 and 11 are indicated for cluster *C3*.

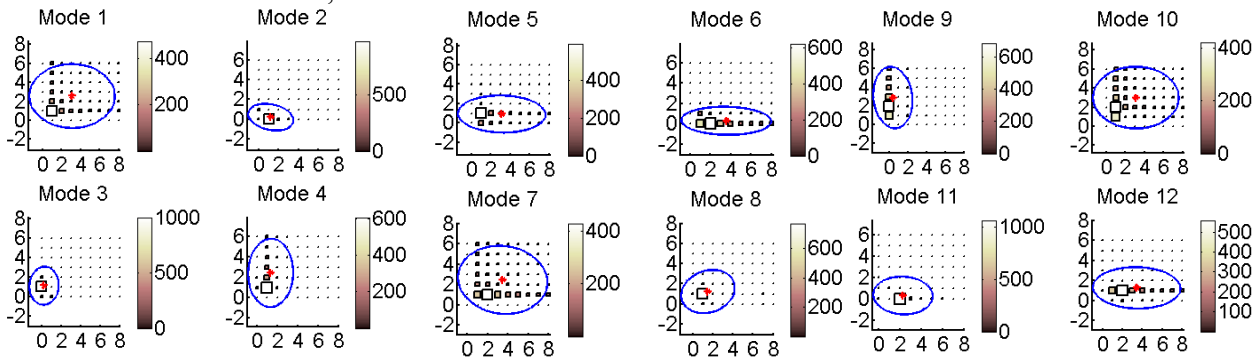


*Fig 6: Non-Negative FD Amplitudes and Elliptical Descriptors of Mode 1-12*

4.3 WD of Rectangular Plate with a Thin Region

A rectangular plate having two regions with different thicknesses was modelled as shown in Fig 9. Four levels of decomposition by the *rbio3.1* wavelet were carried out on the mode shapes of the plate. Thirteen sub-images were obtained for every single mode-shape: 4 horizontal, 4 vertical, 4 diagonal detailed sub-images and 1 approximation sub-image. The average energy of every sub-image was calculated to determine its significance. Fig 10 shows an example of the energy percentage of each sub-image of mode 12. It is noted that the energies are mainly distributed in the higher levels of sub-images. Thus, the original mode shape pattern as shown in Fig 11 can be represented by the wavelet decomposition at level 4. The global shape information can be described by the approximation sub-image and the local shape in the thin region can be detected by the wavelet details which are shown in Fig 12.

Shape feature vector derived by the WD can be constructed by assembling the energy of each sub-

image at different decomposition levels. Global comparison between similar structures can be implemented by the correlations of the approximations. Further details of detecting the thin region and extracting the global pattern by the WDs are described by the present authors [16].

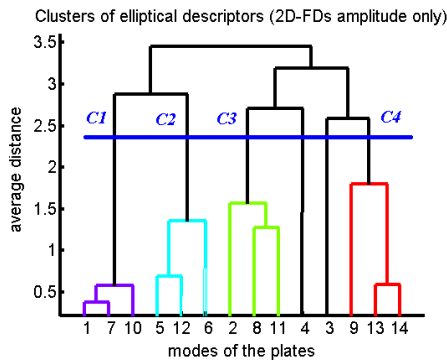


**Fig 7: Dendrogram by Elliptical Descriptor**

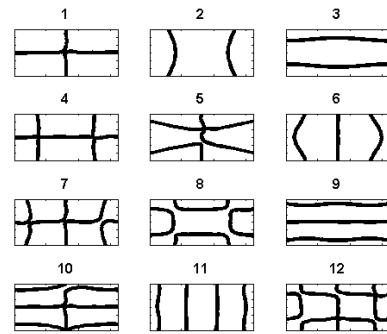


**Fig 8: Nodal Lines of the Rectangular Plate**

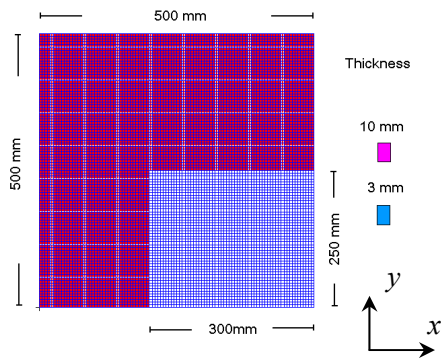


**Fig 9: FE model of Plate pC**

Level	4	3	2	1
4	25.6	24.2	5.9	0.0
	21.1	18.5		
3	2.7		1.1	0.0
2	0.2		0.0	
1	0.0			0.0

**Fig 10: Percentages of Sub-Image Average Energies – Mode 12**

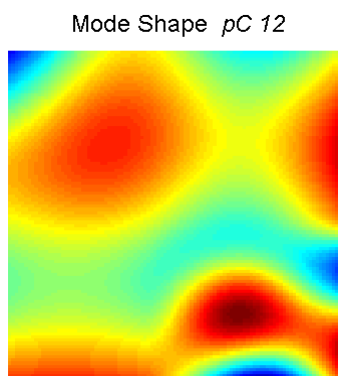


**Fig 11: Mode Shape Pattern**

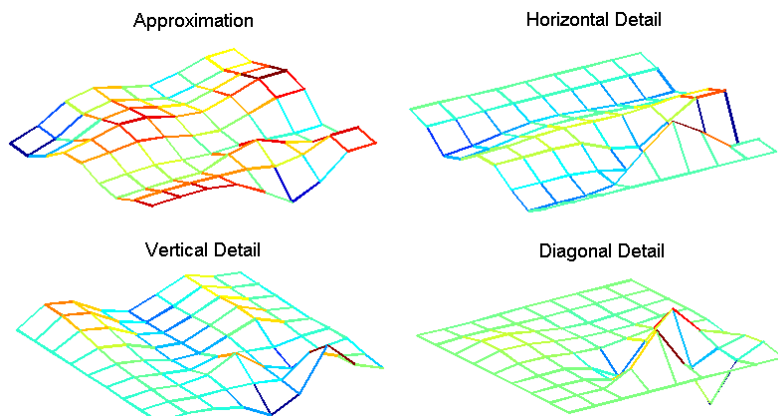


**Fig 12: Decomposition Level 4**

## 5 Conclusion

A variety of shape descriptors which demonstrate the capability of recognising subtle difference in mode shapes are presented. The SDs show the desirable properties of computational efficiency and ease of image reconstruction using a small number of SD terms. Specifically, the ZMD is powerful in discriminating circular and spherical images; the FD is more general and very effective at extracting

mode-shape features by virtue of its sinusoidal kernel; the WD shows the capability of distinguishing between local and global features.

### Acknowledgement

The first author wishes to acknowledge the support of an Overseas Research Studentship (ORS), a University of Liverpool Studentship, an award from the University of Liverpool Graduate Association (Hong Kong) and EC project ADVISE (Advanced Dynamic Validations using Integrated Simulation and Experimentation) Grant 218595.

### References

- [1] A. B. Stanbridge, M. Martarelli, and D. J. Ewins, "Measuring area vibration mode shapes with a continuous-scan LDV," *Measurement*, vol. 35, pp. 181-189, 2004.
- [2] A. K. Jain, R. P. W. Duin, and J. Mao, "Statistical Pattern Recognition: A Review," *IEEE Transactions on Pattern Analysis and Machine Intelligence*, vol. 22, pp. 4-37, 2000.
- [3] L. d. F. Costa and J. R. M. Cesar, *Shape Analysis and Classification Theory and Practice*: CRC Press, 2001.
- [4] R. J. Allemang and D. L. Brown, "A correlation coefficient for modal vector analysis," *Proceeding of 1st International Modal Analysis Conference*, vol. 1, pp. 110-116, 1982.
- [5] D. Zhang and G. Lu, "Review of shape representation and description techniques," *Pattern Recognition*, vol. 37, p. 19, 2004.
- [6] M. R. Teague, "Image analysis via the general theory of moments," *Optical Society of America*, vol. 70, pp. 920-930, 1980.
- [7] C. H. Teh and R. T. Chin, "On image analysis by the methods of moments," *IEEE Transactions on Pattern Analysis and Machine Intelligence*, vol. 10, pp. 496-513, 1988.
- [8] R. J. Prokop and A. P. Reeves, "A survey of moment-based techniques for unoccluded object representation and recognition," *Graphical Models Image Processing*, vol. 54, pp. 438-460, 1992.
- [9] A. Khotanzad and Y. H. Hong, "Invariant image recognition by zernike moments," *IEEE transaction of Pattern Analysis and Machine Intelligence*, vol. 12, pp. 489-498, 1990.
- [10] W. Wang, J. E. Mottershead, and C. Mares, "Mode-shape recognition and finite element model updating using the Zernike moment descriptor," *Mechanical Systems and Signal Processing*, Submitted.
- [11] R. L. Cosgriff, "Identification of Shape," Report No 820-11 of the Ohio State University Research Foundation 1960.
- [12] C. T. Zahn and R. Z. Roskies, "Fourier Descriptors for Plane Closed Curves," *IEEE Transactions on Computers*, vol. C21, pp. 269-281, 1972.
- [13] E. Persoon and K.-S. Fu, "Shape discrimination Using Fourier Descriptors," *IEEE Transactions on Systems Man and Cybernetics*, vol. SMC-7, pp. 170-179, 1977.
- [14] G. Eichmann, "Shape representation by Gabor expansion," *Hybrid Image and Signal Processing II, SPIE*, vol. 1279, pp. 86-94, 1990.
- [15] S. G. Mallat, "A Theory for Multiresolution Signal Decomposition: The Wavelet Representation," *IEEE Transactions on Pattern Analysis and Machine Intelligence*, vol. 11, pp. 674-693, July 1989.
- [16] W. Wang, J. E. Mottershead, and C. Mares, "Vibration mode shape recognition using image processing," *Journal of Sound and Vibration*, submitted.
- [17] F. Zernike, "Translated: diffraction theory of the cut procedure and its improved form, the phase contrast method," *Physica*, vol. 1, 1934.
- [18] P. Hew, "Orthogonal functions on the unit disk having invariance in form," The University of Western Australia 1996.
- [19] I. Daubechies, *Ten Lectures on Wavelets*: SIAM: Society for Industrial and Applied Mathematics, 1992.
- [20] M. I. Friswell and J. E. Mottershead, *Finite Element Model Updating in Structural Dynamics*: Kluwer Academic Publishers, 1995.